

**AUTOMATED POST-EARTHQUAKE DAMAGE ASSESSMENT AND SAFETY
EVALUATION OF INSTRUMENTED BUILDINGS**

Farzad Naeim, Scott Hagie and Arzhang Alimoradi

John A. Martin and Associates, Inc.

Eduardo Miranda

Stanford University

Abstract

A set of methodologies for automated post earthquake damage assessment of instrumented buildings are presented. These methods can be used immediately after an earthquake to assess the probability of various damage states in the N-S and E-W directions and throughout the height of each building. The methods have been applied to more than 40 CSMIP instrumented buildings which have recordings from more than one earthquake. The results indicate that the proposed methods, when used in combination, can provide very useful information regarding the status of a building immediately after an earthquake by simple and rapid analysis of sensor data and prior to any building inspections.

Introduction

This paper provides an overview of an exhaustive investigation to determine the feasibility of an automated approach to post-earthquake damage assessment of instrumented buildings and establishment of a coherent set of techniques and methodologies to achieve the objective of automated post-earthquake damage assessment.

The objective of this project was to use and study strong-motion data from instrumented buildings with several earthquake records to determine the threshold of measures of motion that would provide guidance to the building officials, in a manner consistent with ATC-20, for determining whether to inspect the building or evacuate it based on the records taken from the building. The proposed measures are such that they can be computed directly from recorded data of instrumented buildings.

Due to publication space constraints this paper provides only a preview of the methodologies developed and a small number of representative examples. A full report which is currently in preparation (Naeim et. al, 2005) will contain detailed information regarding various methodologies implemented and the results of application to numerous instrumented buildings. In addition, papers are being prepared for submission to scientific journals that document certain

major developments achieved during this project (Alimoradi, et. al 2005a; Alimoradi et. al, 2005b).

Automated damage assessment (ADA) provides an incentive for building owners to instrument their buildings and has the potential of significantly adding to the inventory of instrumented buildings so critically needed for development and evaluation of existing and future design provisions. Elimination or reduction of possible false alarms produced by ADA procedures is a major concern. Therefore, we assess damage using several independent techniques and provide the degree of confidence in terms of probability of occurrence with each of our damage assessments.

Robust ADA methodologies should be able to provide increasingly more accurate estimates of post-earthquake damage when more information is available regarding the building and its contents. With our approach, preliminary damage estimates are provided based on the sensor data and a general understanding of the building and its contents. More accurate damage estimates may be obtained if more detailed information regarding the structural system and contents are available such as detailed fragility curves for various components.

The more specific information ADA provides, the more useful it is. We provide damage estimates per floor in each direction of the building. Damage estimates may be based on the maximum response values per floor or response values at the geometric center of each floor's diaphragm.

In more ways than one this project is a natural continuation of the last year's effort which resulted in development and dissemination of the CSMIP-3DV software system (Naeim, et. al, 1994). We utilized and expanded on the information that we generated regarding 80 CSMIP instrumented buildings contained in the CSMIP-3DV database in order to evaluate, rank, and combine various potential methods to achieve reliable automated post-earthquake damage detection. These enhancements include:

- Calculation of instantaneous and envelope values of story forces and story shears, as well as hysteretic diagrams for these parameters.
- Calculation of instantaneous and envelope values of floor accelerations, velocities and floor spectral attributes.
- Application of numerous fragility curves (Aslani and Miranda 2003; FEMA 2004; Porter and Kiremidjian 2001) for probabilistic assessment of damage to structural and nonstructural systems and components.
- Investigation of possible use of FEMA-356 (ASCE 2000) tables and/or linear/nonlinear response analyses for damage assessment.
- Investigation of the use of Wavelet Analysis techniques for damage assessment
- Development of a new rapid system identification technique based on the use of Genetic Algorithms (Alimoradi, et. al 2005a) and approximate mode shapes (Miranda and

Taghavi 2005; Alimoradi, et. al 2005b) for identifying building periods, mode shapes, and changes in dynamic characteristics of buildings during their response to earthquake ground motions.

- Investigation of the use of the Fuzzy Logic Theory (Revadigar and Mau 1999) for combining information obtained from various methods and techniques.

Classes of Potential Damage Indicator Parameters

Several categories of techniques for automated damage assessment based on building records were evaluated:

1. “Simple” or “Design Oriented” Measures. These include demand/capacity ratios based on the following measures.
 - a. Comparison of base shear inferred from the records with the capacity level values suggested by the applicable code or used in design.
 - b. Comparison of maximum inter-story drifts inferred from records with the capacity level values suggested by the applicable code or used in design.
 - c. Comparison of observed peak ground acceleration obtained from the records with the capacity level values suggested by the applicable code or used in design.
 - d. Comparison of relevant response spectral entities for a number of modes, combined using an appropriate spectral combination technique, with the capacity level values suggested by the applicable code or used in design.
2. Probability-based Measures. These include the fragility functions developed by PEER/NSF, utilized by HAZUS-MH and proposed by Porter and Kiremidjian as well as an attempt to cast FEMA-356 limit-state tables in a pseudo fragility function form for possible damage assessment. These are probabilistic damage measures for various floors and contents which are developed utilizing one or more of the following indicators:
 - a. Peak inter-story drift ratios
 - b. Peak floor accelerations
 - c. Peak floor velocities
 - d. Floor response spectra
 - e. Story shears inferred from recorded motions
3. Wavelet Characteristic Measures. These are signal processing measures based on wavelet analyses in which the high-frequency content of the signal is separated from its low frequency content in order to provide information on the timing and extent of changes in the frequency and amplitude characteristics of the sensor data.
4. Damage Measures Based on Structural Identification. These are damage measures

inferred from changes in the dynamic characteristics of the building such as elongation of natural periods or a change in the dominant mode of behavior of the building during an earthquake (i.e., a change from shear dominated deformation shape to a flexural dominated shape or vice versa).

Consistent with ATC-20 (Applied Technology Council, 1989), the damage state suggested by each damage indicator are classified in one of the following four categories:

1. No Damage
2. Slight Damage
3. Moderate Damage
4. Severe Damage

Use of Fragility Curves for Damage Assessment

As will be shown later in this paper, the various fragility curves proved to be the most useful tools for post-earthquake damage assessment. Once engineering demand parameters have been computed based on interpreted data from the sensors, damage in specific stories can be estimated through the use of fragility functions. A fragility function relates structural response with various levels of damage. Unlike deterministic values recommended in FEMA-356 (ASCE, 2000), fragility functions take into account the uncertainty on the structural motions that trigger different levels of damage. In particular, a fragility function supplies the probability that the structure will reach or exceed a particular damage level.

Available experimental data on various types of structural components permit the development of fragility functions. Recent research at PEER (Aslani and Miranda, 2003) indicates that fragility functions for many structural components can be assumed to follow a lognormal distribution. Fragility curves implemented in HAZUS also utilize a lognormal shape. Examples of probabilities of experiencing light (dm_1) and severe (dm_2) cracking in reinforced concrete slab-column connections as a function of interstory drift ratio are shown in Figure 1.

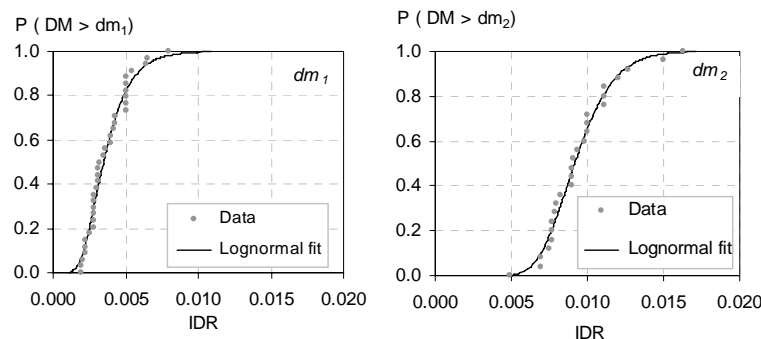


Figure 1. Example of fragility functions to estimate damage in reinforced concrete buildings with slab-column connections as a function of interstory drift (After Aslani and Miranda, 2003).

As shown in this figure severe cracking in slab-columns connections has been observed in specimens subjected to interstory drift ratios as low as 0.5% while in others as large as 1.6%.

Rather than categorically stating that severe cracking occurs at a particular level of interstory drift, fragility functions describe how the probability of reaching or exceeding this level of damage increases as the interstory drift ratio imposed in the building increases. As shown in the figures the lognormal distribution captures quite well the observations from experimental results.

Fragility functions assumed to follow a lognormal probability distribution are defined by only two parameters for each damage state. One parameter describes the engineering demand parameter at which a 50% probability of reaching or exceeding a damage state occurs and the other parameter describes the dispersion in the data. An example of fragility functions for three damage states is presented in Figure 2.

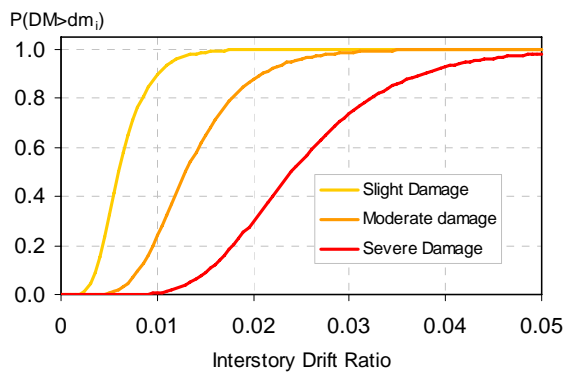


Figure 2. Example of drift-based fragility functions for three damage states.

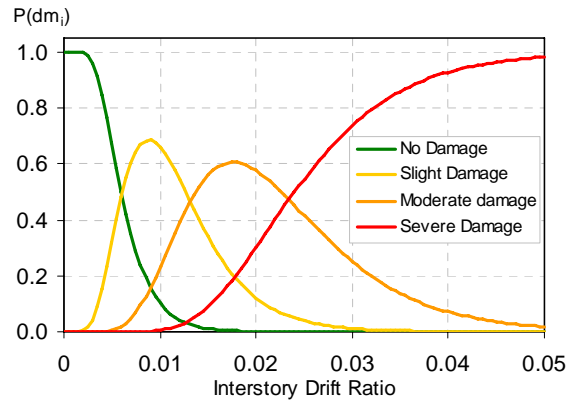


Figure 3. Probabilities of being in various damage states as a function of the level of interstory drift demand.

Once the fragility functions have been defined, the probability of being in one of the damage states is easily computed as the difference between two consecutive damage states. An example of damage being within one of the various damage states is shown in Figure 3.

It can be seen that, for this example, stories with interstory drift demands of 1% would have a very small probability (about 10%) of not having damage, a high probability of having slight damage (about 65%), a small probability of experiencing moderate damage (about 20%) and essentially no chance of experiencing severe damage. However, stories experiencing an interstory drift demand of 2.5% would certainly experience some degree of damage: about 5% probability that the damage is slight, about 40% that is moderate and about 55% of experiencing severe damage.

The fragility-based damage assessment algorithms provide the decision makers with a number of options for estimating structural and nonstructural damage in a CSMIP-instrumented building:

- 1) Apply the HAZUS-MH fragility functions for various FEMA categories of buildings and regions
- 2) Apply the PEER/NSF fragility functions or fragility functions provided by other researchers

- 3) Use the deterministic values provided by FEMA-356; or
- 4) Use their own fragility functions obtained from detailed structural analyses of the building performed prior to the earthquake(s).

Examples

An overview of the utility and limitations of various ADA techniques evaluated and implemented during this study are provided by examination of two instrumented buildings. Details of application to other buildings will be included in our final report to CSMIP (Naeim, et al, 2005). The two selected building examples are:

1. The Imperial Valley County Services Building response to the 1979 Imperial Valley earthquake, and
2. The Van Nuys 7 Story Hotel response to the 1992 Landers and Big Bear, and the 1994 Northridge earthquakes.

Example 1. Imperial Valley County Services Building (CSMIP ID = 01260)

This six story building has been the subject of numerous studies (Figure 4a). A reinforced concrete building with discontinuous shear walls, it suffered severe damage in the form of collapse of the first floor concrete columns at the ground floor during the 1979 Imperial Valley earthquake (Figure 4b). The building was subsequently demolished. The irregular structural system, interruption of exterior walls at the second floor, and sudden transfer of loads at that plane were major contributors to the failure of this building. A sketch of the building depicting sensor locations is shown in Figure 5.

System identification using GA optimization in the East-West direction indicates that the initial fundamental period of this building was about 0.7 sec. This period was elongated to 1.5 sec. towards the end of the record (Figure 6). Comparison of input elastic spectra at the base with a typical unreduced code spectrum for seismic zone 3, where this building was located, provides little to work with as far as damage assessments are concerned (see Figure 7). First, the elastic demand/capacity ratios in the E-W and N-S directions look about the same. Second, comparison of modal base shear demand and assumed capacities are not far apart from each other. Third, no information pertaining to the significant attributes of the building particular to this structure, such as irregularity, discontinuity of shear walls can be inferred from spectral comparisons. Fourth, the E-W and N-S picture do not vary by much although the building is significantly weaker in the E-W direction. Finally, no information regarding the possible distribution of damage throughout the height of the structure can be obtained from Figure 7. This illustrates the disadvantages of using design-based approaches as tools for automated post-earthquake damage assessment.

Instantaneous and maximum values of interstory drifts of CSMIP instrumented buildings after an earthquake can be easily and immediately estimated using tools such as CSMIP-3DV (Naeim et. al, 2004). These drift values were proven to be of immense value in automated damage assessment. A glimpse at the E-W and N-S lateral displacements and story drifts (Figures 8 and 9) reveals that the drift demands in the E-W direction were significantly larger

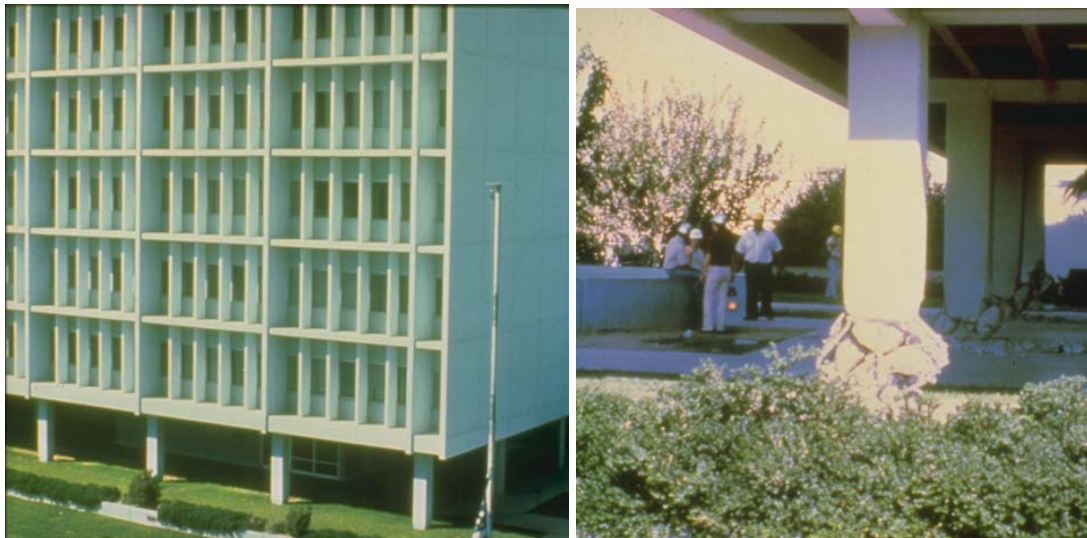
than those in the N-S direction. Furthermore, a drift of 3.5 inches at the first floor is inferred from sensor data in the E-W direction while the maximum drifts in the upper floors are limited to about 1.0 inch. Evaluation of the shear-displacement hysteretic plots (Figure 10) indicates significantly larger excursions and softening of the first floor in the E-W direction.

Surprisingly, completely independent approaches using interstory drift indices provide similar and very useful results. For example, if we use HAZUS-MH fragility curves based on interstory drifts for this type of building (C1M or C2M, older building), we obtain 85% probability of severe damage and 15% probability of moderate damage at the first floor in the E-W direction (see Figure 11). This is exactly where the column failures occurred. In the N-S direction at the same floor the probability of severe damage is estimated at less than 11% and probability of moderate damage at 78%. The damage at the upper floors of this building was limited as the failure of the first floor columns produced a relatively rigid pin-based block. This is also reflected in these damage estimates. In the E-W direction the probabilities of severe, moderate, slight and no damage are constant from the second floor to roof at 6%, 76%, 16% and 1%, respectively. In the N-S direction these values are 0%, 11%, 47%, and 42% respectively.

Use of the PEER/NSF fragility curves for flexural behavior of nonductile R/C columns provides similar useful information (see Figure 12). Based on this approach, the probability of severe damage to the first floor columns in the E-W direction is 74% and in the N-S direction is 19%. The probability of the severe column damage in upper floors is only 14% in the E-W direction and 0% in the N-S direction. The elegance of the PEER/NSF fragility curves is that the probability of damage based on various damage mechanisms and various components can be estimated. For example, using the fragility curves developed for old R/C beam-column joints, one obtains that the probability for beam-column joint severe damage throughout this building is 0% while the probability of slight damage to these joints is 81% at the first floor in the E-W direction.

Even FEMA-356 tables intended for nonlinear performance analyses such as Table 6-8 can be cast into a fragility curve for the purposes of automated post-earthquake damage assessment. For example, one can assume a certain level of elastic drift and apply some adjustment factors to take into consideration the inherent conservatism of FEMA-356 tabulated limit states. For instance, if we assume the building can take 0.005 of interstory drift angle within its elastic limit, do not apply any adjustment factors, and use the mean secondary values provided in FEMA-356 Table 6-8 for nonconforming columns in flexure (see Figure 13), then our damage assessment would indicate a 100% probability of exceeding the secondary Collapse Prevention (CP-S) for the first floor columns in the E-W direction (Figure 14). Based on this analysis, all columns in upper floors are within the Immediate Occupancy (IO) limit state.

In summary, use of sensor data to estimate interstory drifts and application of various fragility curves, if available at the time, could have provided excellent post-earthquake damage assessment of this building.



(a) A view of the building

(b) Failure of columns at the base

Figure 4. Imperial County Services Building (Photo Credits: BAREPP and USGS)

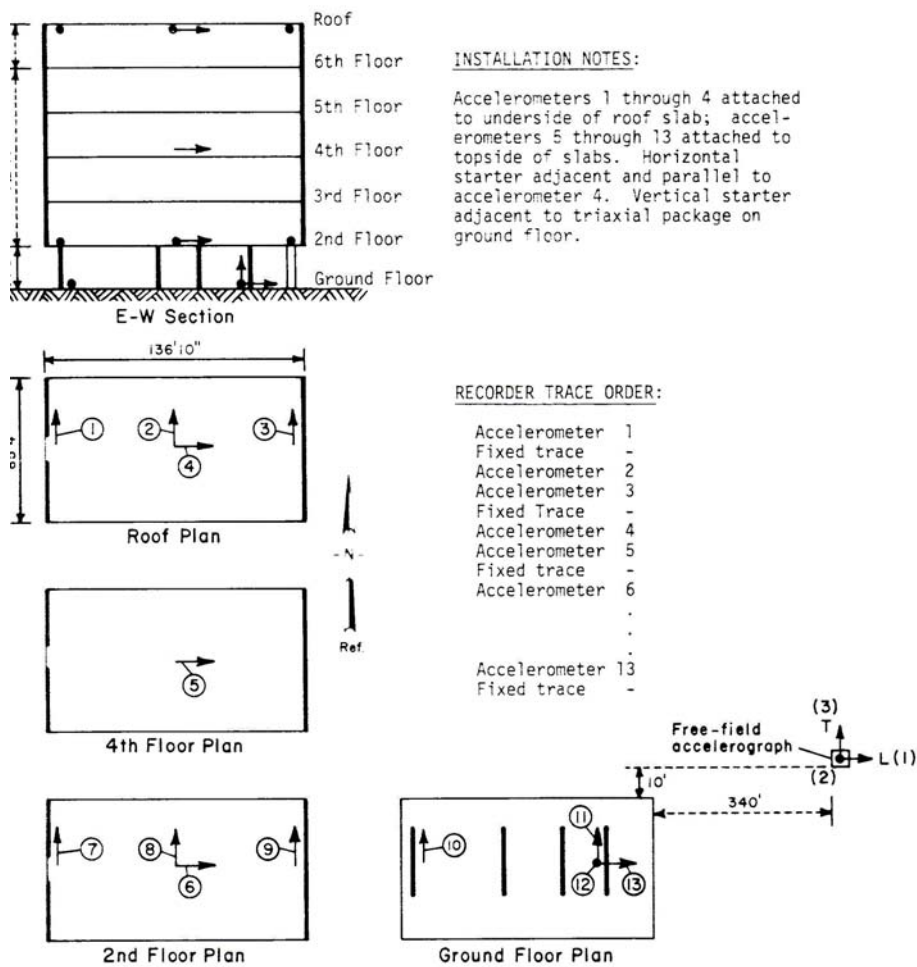


Figure 5. Sketch and sensor layout for Imperial County Services Building (from McJunkin and Ragsdale 1980)

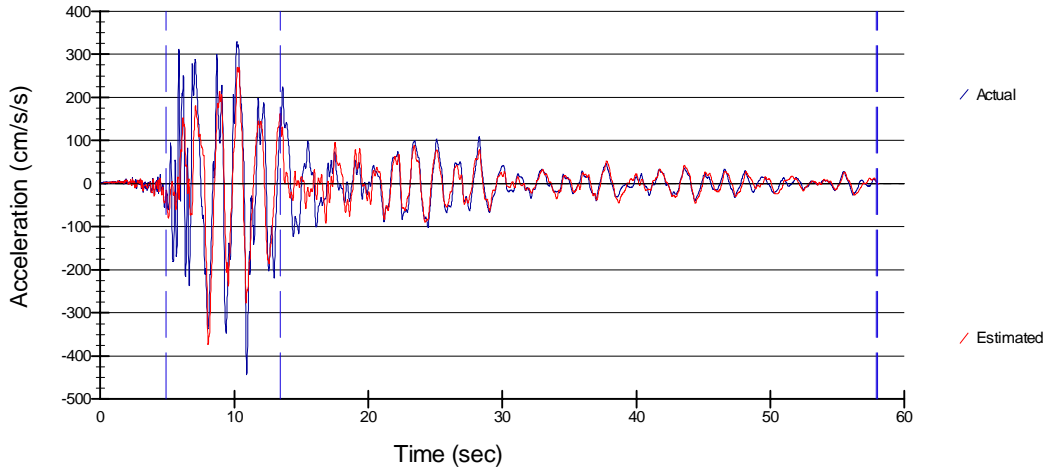


Figure 6. Recorded and GA identified response in the E-W direction at the roof.

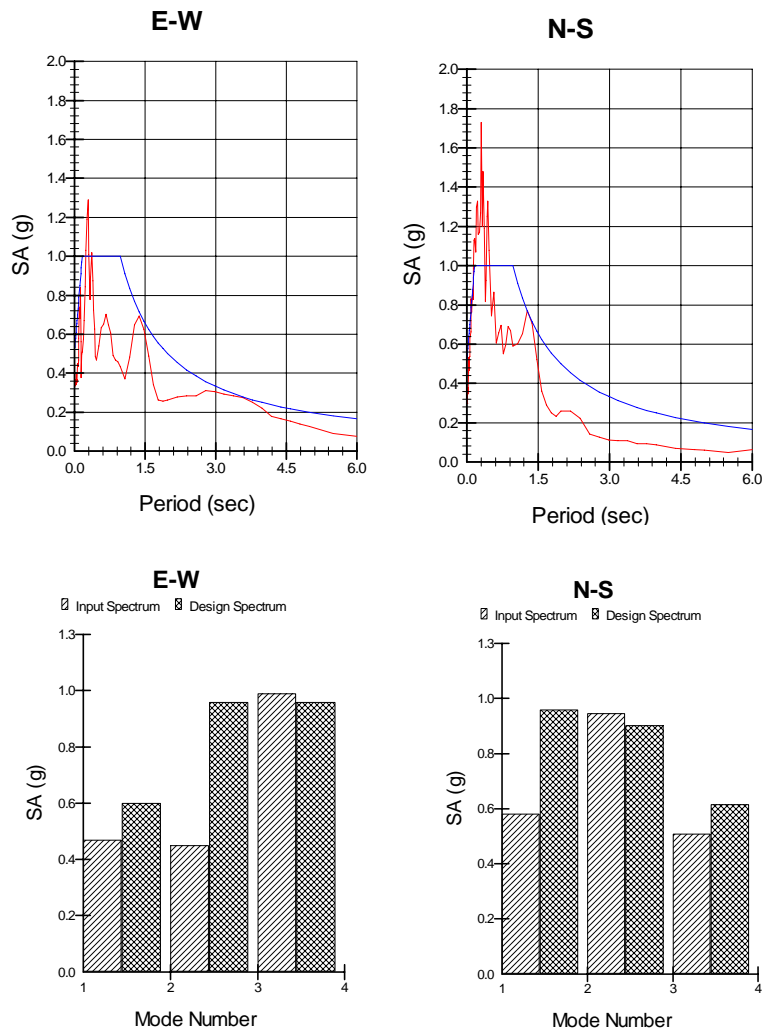


Figure 7. Comparison of the recorded response spectra (5% damped) at the base of the building with a typical "design" spectrum for seismic zone 3 and corresponding elastic modal demands for modes 1 to 3.

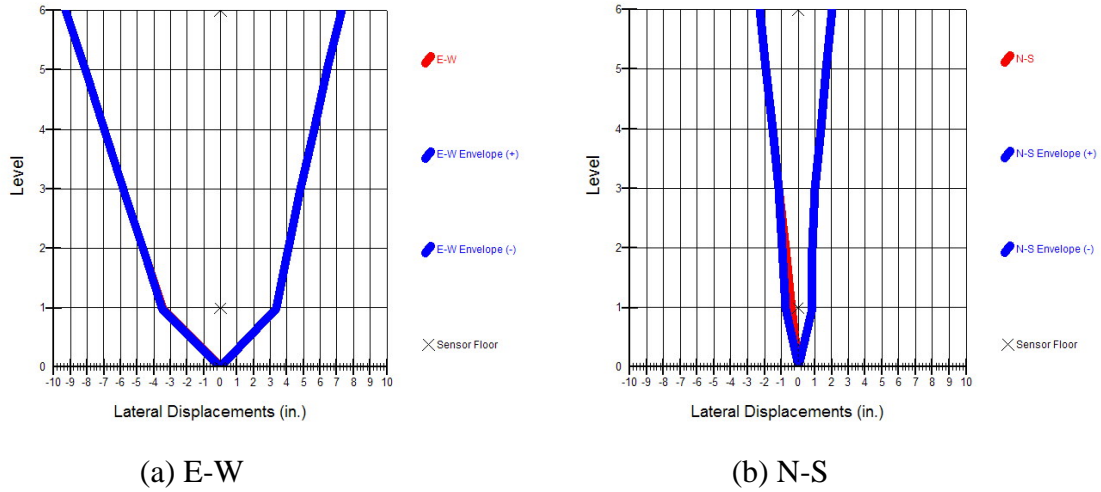


Figure 8. Maximum lateral displacements in the E-W and N-S directions

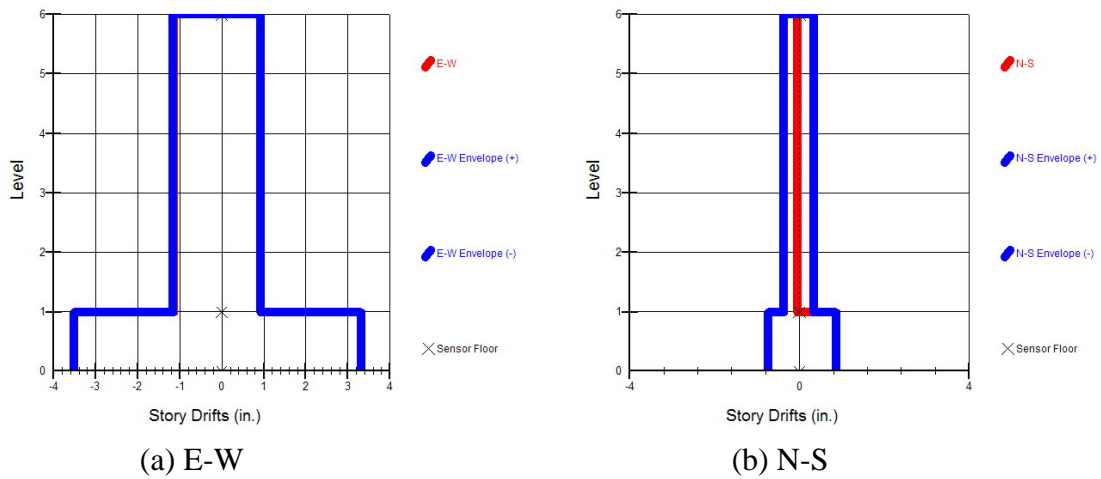


Figure 9. Maximum interstory drifts in the E-W and N-S directions

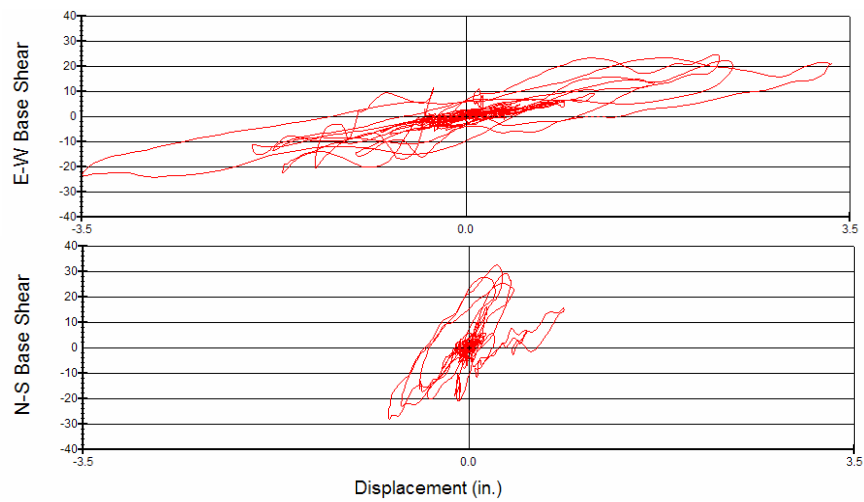


Figure 10. First floor shear-displacement hysteretic loops (E-W on top, N-S at the bottom)



Figure 11. Damage probability established based on HAZUS-MH drift-based fragility curves for older concrete buildings clearly identifies the first floor in the E-W direction as the zone of severe damage.

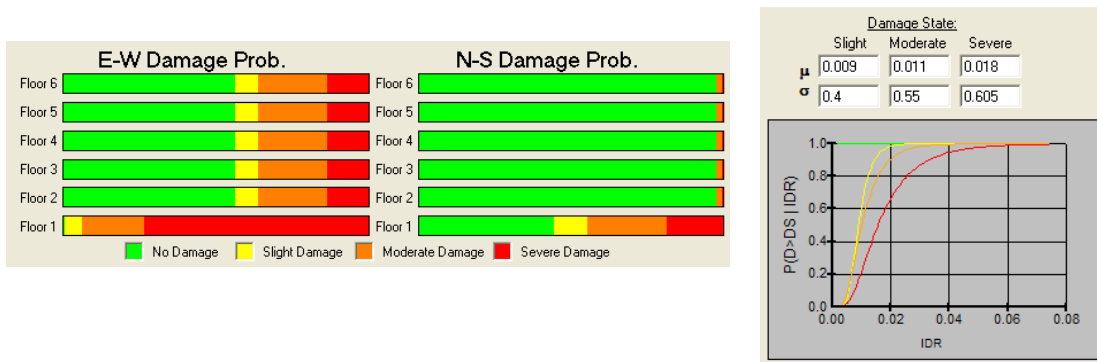


Figure 12. Damage probability established based on PEER/NSF fragility curves for nonductile R/C columns under large gravity loads clearly identifies the first floor columns in the E-W direction as the zone of severe damage.

Figure 13 shows the assumptions used in converting FEMA-356 tabulated values to a fragility curve for nonductile R/C columns. The dialog box includes the following fields:

- Component: Column
- Action: Flexure
- Elastic Rotation: 0.005 Radians
- SD-1 Limit State ID: Immediate Occupancy
- SD-2 Limit State ID: Life Safety (Secondary)
- SD-3 Limit State ID: Collapse Prevention (Secondary)
- Plastic Rotation Associated with Each Damage State:

	SD-1	SD-2	SD-3	
Low:	0.002	0.005	0.008	Radians
High:	0.005	0.01	0.015	Radians
- Adjustment Factor: 1, 1, 1

Figure 13. Assumptions used in converting FEMA-356 tabulated values to a fragility curve for nonductile R/C columns

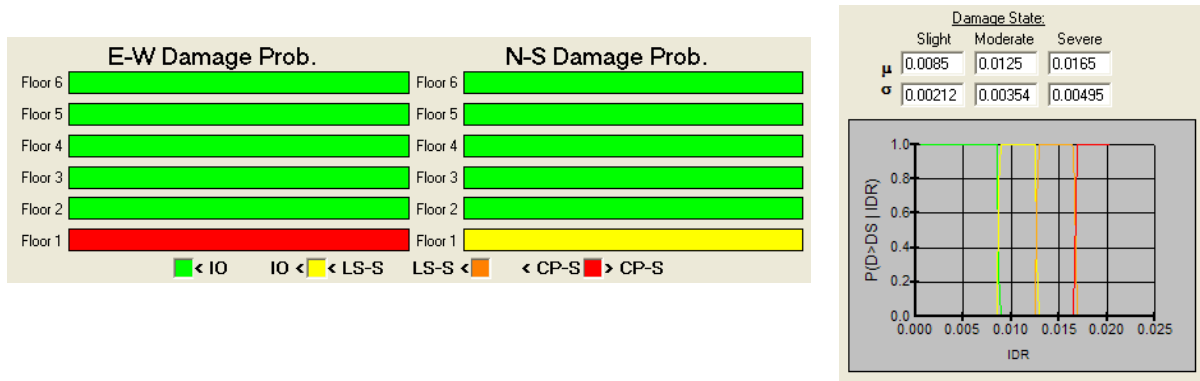


Figure 14. Damage probability established using Tables contained in FEMA-356 for limit-states of nonductile concrete columns clearly identifies the first floor in the E-W direction as the zone of severe damage.

Example 2. The Van Nuys 7-Story Hotel (CSMIP ID = 24386)

This 7-story nonductile concrete frame building (Figures 15 and 16) is probably the most studied instrumented building in the world. We applied ADA to records obtained from three earthquakes: 1992 Landers, 1992 Big Bear, and 1994 Northridge earthquake. The building did not suffer damage during the 1992 events but did suffer significant structural damage during the 1994 Northridge earthquake in the form of shear failure of columns at the 4th floor on the exterior E-W frame on the south face of the building.

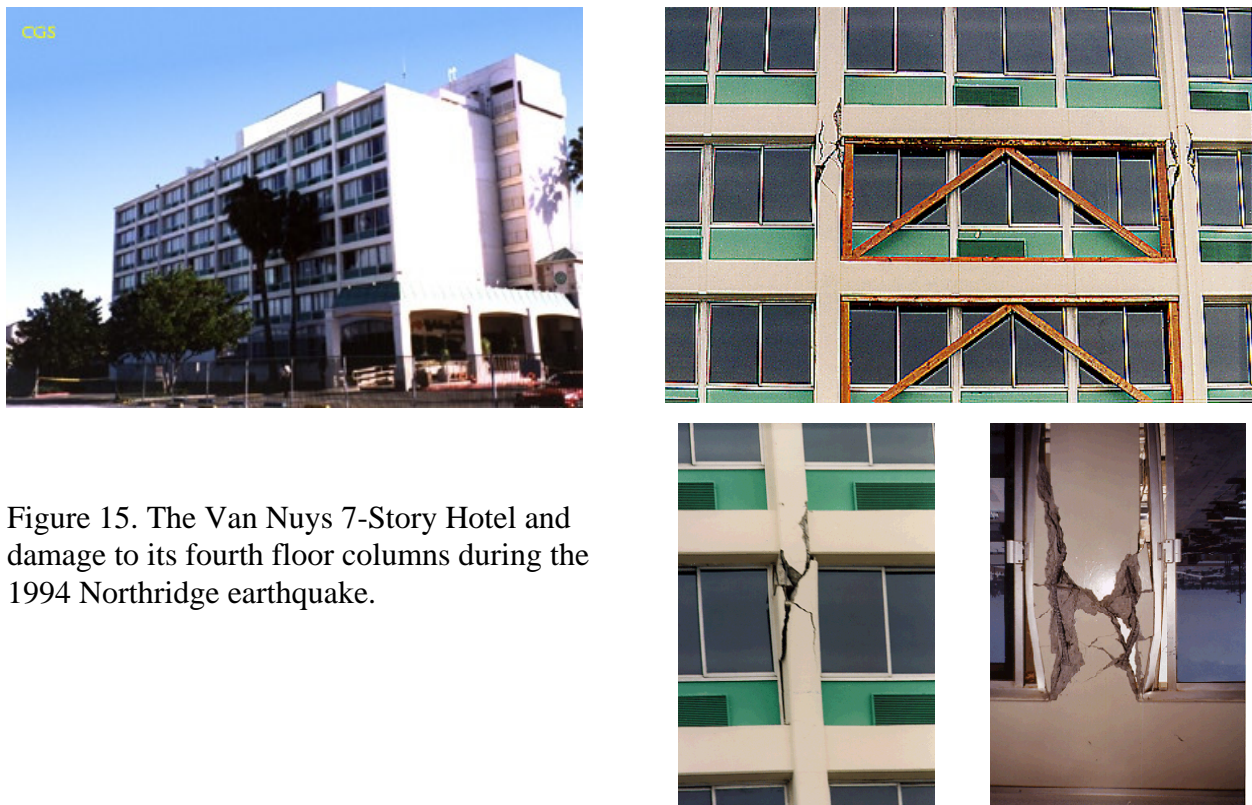


Figure 15. The Van Nuys 7-Story Hotel and damage to its fourth floor columns during the 1994 Northridge earthquake.

Van Nuys - 7-story Hotel
(CSMIP Station No. 24386)

SENSOR LOCATIONS

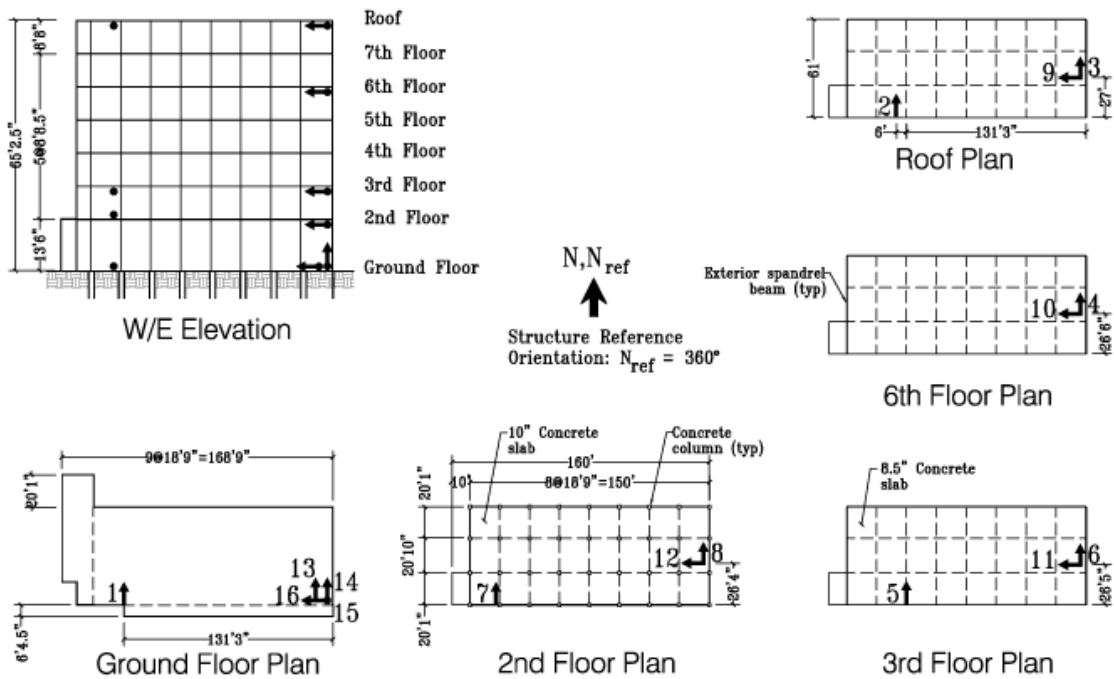


Figure 16. Sketch and sensor layout for the Van Nuys 7 Story Hotel.

Fragility analysis for 1992 Landers and Big Bear earthquakes using HAZUS-MH, PEER/NFS and FEMA-356 parameters all indicate that this building did not suffer structural damage during these two earthquakes (See Figure 17 for an example). The picture, however, is entirely different for the 1994 Northridge earthquake where all three methods indicate a high probability of extensive damage to the middle floors of the building (Figures 18 and 19). Please note that contrary to the Imperial Valley Services Building, no sensors were installed in this building on the floor that was damaged. Therefore, the estimates are provided by interpolation between sensors at other floors. As a result the ADA procedures assign possibility of damage to several floors in the building and cannot pinpoint the exact floor at which the damage occurs.

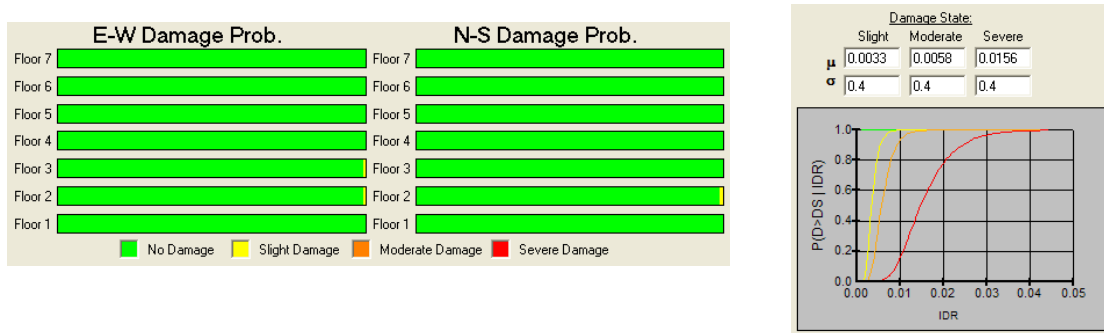


Figure 17. Damage probability established based on HAZUS-MH drift-based fragility curves for older concrete buildings indicates no damage during the Big Bear and Landers earthquakes.

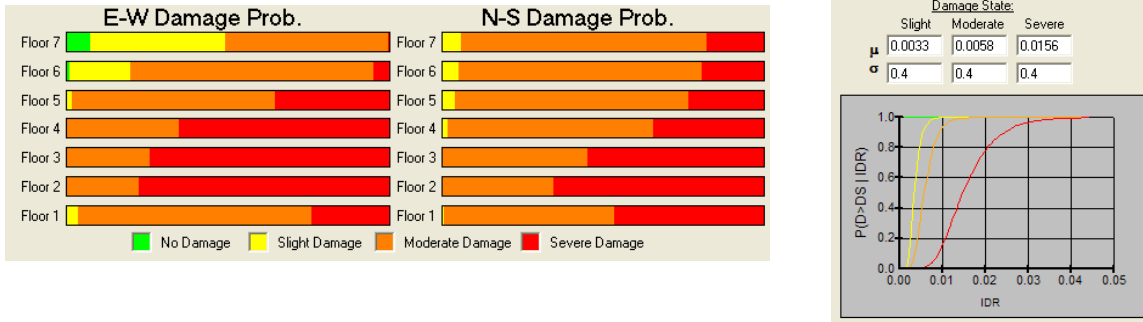


Figure 18. Damage probabilities established based on HAZUS-MH drift-based fragility curves for the 1994 Northridge earthquake show 100% probability of moderate to severe damage at the second to fourth floors.

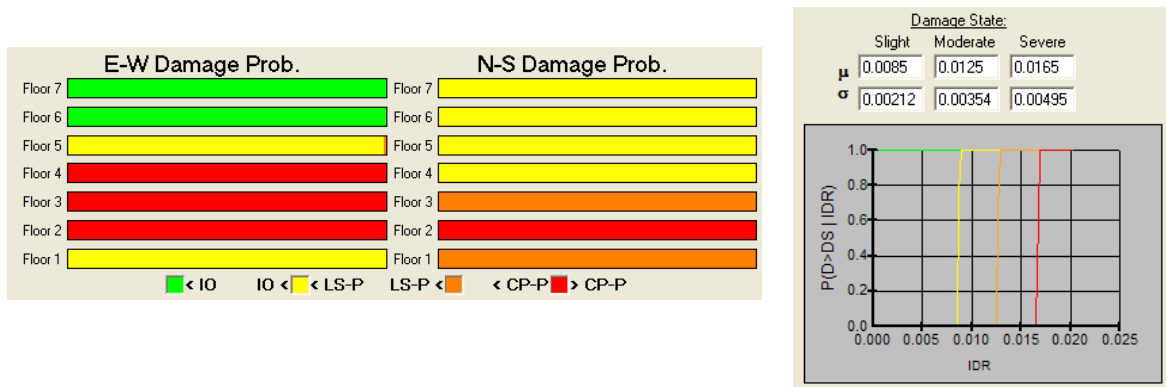


Figure 19. Damage probabilities established using FEMA-356 Tables indicate 100% probability of exceeding Collapse Prevention limit state at second to fourth floors in the E-W direction.

Our experience indicates that wavelet analysis shows promise if the results of wavelet analysis details are compared to those obtained from an earthquake in which the building was known to be not damaged (baseline earthquake). Otherwise, the possibility of false alarms based on wavelet analysis is high. Here, we use 1992 Big Bear as the baseline earthquake to estimate damage probability during the 1994 Northridge earthquake.

The amplitudes and details of wavelet analysis using a DB4 wavelet for various sensors are shown in Figure 20 where it can be seen that the detail content for the Northridge event is significantly richer than the corresponding details for the Big Bear event. Application of a simple fragility curve based on wavelet detail ratios obtained from several buildings with observed damage and the corresponding damage probabilities for the 1994 Northridge earthquake are shown in Figure 21. Notice that this procedure identifies the location of a virtual sensor at the 4th floor with the highest probability of damage at 92%. The results shown at the bottom for sensors 1 and 14 should be ignored because these are input sensors at the ground level. Unfortunately, obtaining more detailed damage estimates in terms of extent of damage (i.e., slight, moderate, severe) from wavelet analysis alone does not seem possible at this time.

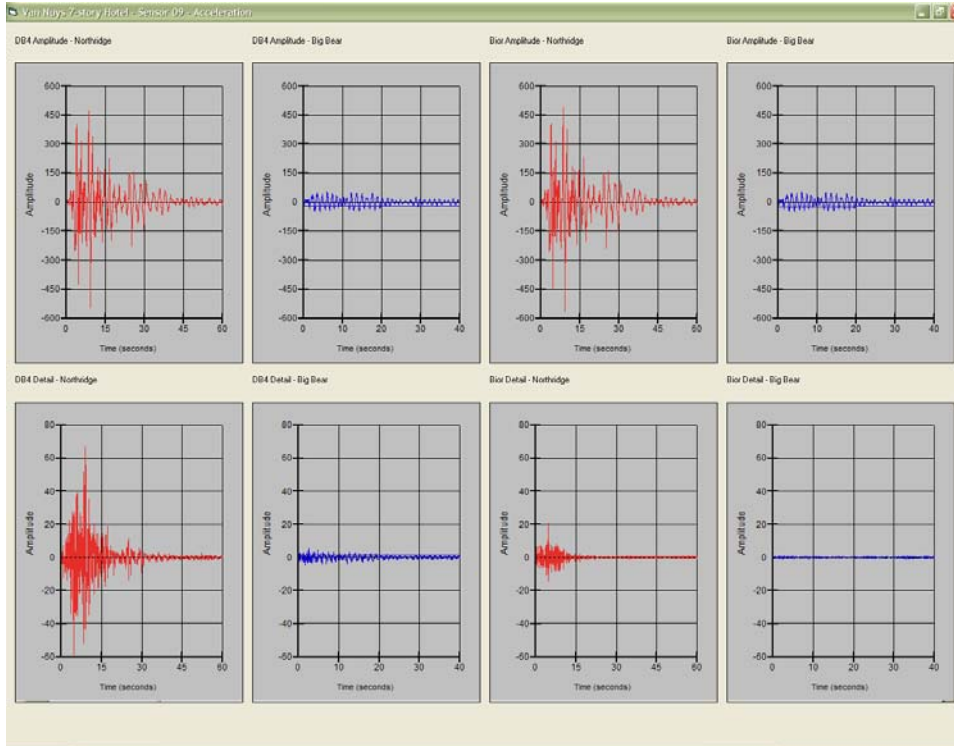


Figure 20. Amplitudes (top) and details (bottom) for a DB4 wavelet analysis of sensor data for the 1994 Northridge and the 1992 Big Bear earthquakes.

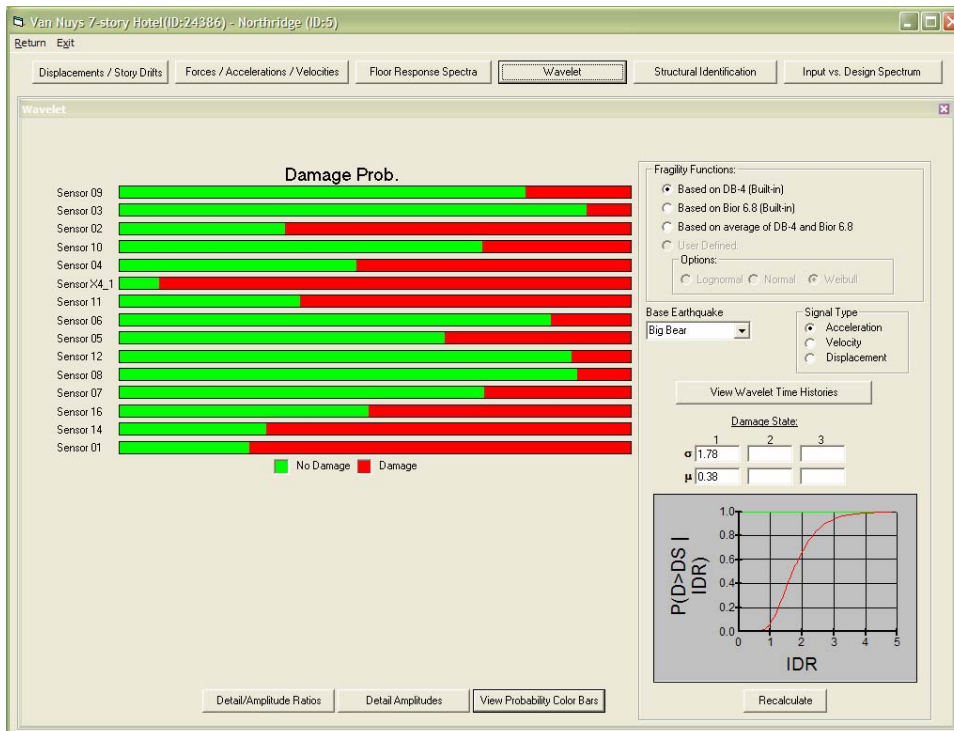


Figure 21. Damage probabilities obtained by wavelet analysis for the 1994 Northridge earthquake.

Conclusions

A set of methodologies for automated post earthquake damage assessment of instrumented buildings were presented. It was shown that these methods can be used immediately after an earthquake to assess the probability of various damage states in the N-S and E-W directions and throughout the height of each building. The methods have been applied to more than 40 CSMIP instrumented buildings which have recordings from more than one earthquake. The results indicate that the proposed methods can provide extremely useful information regarding the status of a building immediately after an earthquake by simple and rapid analysis of sensor data and prior to any building inspections.

Acknowledgments

Funding for this project was provided by State of California, California Geologic Survey, Strong Motion Instrumentation Program (SMIP) under Contract Number 1003-781.

The authors wish to express their gratitude to the members of the consulting panel of experts consisting of Professors Wilfred Iwan, S.T. Mau, and Eduardo Miranda.

The opinions expressed in this paper are those of the author and do not necessarily reflect the views of the California Strong Motion Instrumentation Program or John A. Martin and Associates, Inc.

References

- Alimoardi, A., and Naeim, F., 2005a, *Identification of Linear and Nonlinear Seismic Response using Genetic Algorithms*, in preparation.
- Alimoardi, A., Miranda, E., Taghavi, S, and Naeim, F., 2005b, *Automated Identification of Linear and Nonlinear Structural Systems using Genetic Algorithms and Approximate Mode Shapes*, in preparation.
- American Society of Civil Engineers (ASCE), 2000, *Prestandard and Commentary for the Seismic Rehabilitation of Buildings*, Washington, D.C.
- Applied Technology Council (ATC), 1989, *Procedures for Postearthquake Safety Evaluation of Buildings*, Redwood City, CA.
- Aslani, H., and Miranda, E., 2003, "Probabilistic Assessment of Building Response During Earthquakes," in *Applications of Statistics and Probability in Civil Engineering*, Der Kiureghian, Madanat and Pestana (eds), Millpress, Rotterdam.
- California Strong Motion Instrumentation Program (CSMIP), 1995, *Processed Data for Los Angeles 2-story Fire Command Control Building from the Northridge Earthquake of 17 January 1994*, Report No. OSMS 95-01A.
- Federal Emergency Management Agency (FEMA), 2004, *HAZUS-MH Technical Manual*, Washington, D.C.
- McJunkin, R.D., and Ragsdale, J.T., 1980, *Compilation of Strong Motion Records and*

Preliminary Data from the Imperial Valley Earthquake of 15 October 1979, Preliminary Report 26, Office of Strong Motion Studies, California Division of Mines and Geology, Sacramento, CA.

Miranda E., and Taghavi S., (2005) "Approximate Floor Acceleration Demands in Multistory Buildings: I Formulation," *Journal of Structural Engineering*, Vol. 131, No. 2, pp. 203-211, American Society of Civil Engineers.

Naeim, Farzad, 1997, *Performance of 20 Extensively Instrumented Buildings during the 1994 Northridge Earthquake – An Interactive Information System*, A report to CSMIP, John A. Martin & Associates, Inc.

Naeim, F., Lee, H., Bhatia, H., Hagie, H., and Skliros, K., 2004, "CSMIP Instrumented Building Response Analysis And 3-D Visualization System (CSMIP-3DV)," *Proceedings of the SMIP-2004 Seminar*.

Naeim, F., H., Hagie, H., Alimoradi, A., and Skliros, K., 2005, *Automated Post-Earthquake Damage Assessment and Safety Evaluation of Instrumented Buildings*, A report to CSMIP, John A. Martin & Associates, Inc., in preparation.

Porter and Kiremidjian, 2001, *Assembly-Based Vulnerability of Buildings and its Uses in Seismic Performance Evaluation and Risk-Management Decision-Making*, Report No. 139, John A. Blume Earthquake Engineering Research Center, Stanford, CA

Revadigar, S. and Mau, S.T., "Automated Multi-criterion Building Damage Assessment from Seismic Data," *Journal of Structural Engineering*, ASCE, Vol. 125, No. 2, Feb., 1999, pp. 211-217.

